Improving Graphene Conductivity through Selective Atomic Layer Deposition

To cite this article: Chanyuan Liu *et al* 2015 *ECS Trans.* **69** 133

View the article online for updates and enhancements.

You may also like

- Graphene devices with bottom-up contacts by area-selective atomic layer deposition
Nick F W Thissen, René H J Vervuurt, Adriaan J M Mackus et al.
- Atomic layer deposited oxide films as protective interface layers for integrated graphene transfer
A Cabrero-Vilatela, J A Alexander-Webber, A A Sagade et al.
- Thin and Uniform Atomic Layer Deposited ZrO_2 Film on Functionalization Graphene
Jeong Woo Shin, Myung Hoon Kang, Seongkook Oh et al.

This content was downloaded from IP address 130.132.173.20 on 28/09/2026 at 18:12

ECS Transactions, 69 (7) 133-138 (2015)
10.1149/06907.0133ecst ©The Electrochemical Society

Improving graphene conductivity through selective atomic layer deposition

Chanyuan Liu[a,b#], Xiaogang Han[a#], Wenzhong Bao[a], Alex Pearse[a,b], Liangbing Hu[a*], Gary Rubloff[a,b*]

[a]Department of Materials Science and Engineering, University of Maryland, College Park, Maryland 20742, USA,
[b]Institute for Systems Research, University of Maryland, College Park, Maryland 20742, USA,
# These authors contributed equally to this work
*email: bingbu@umd.edu, rubloff@umd.edu

Abstract

We present a method to electrically heal and connect graphene flakes via selective atomic layer deposition (ALD) of conductive materials. Selective growth of conductive materials is observed on graphene cracks and edges but exhibits a significant nucleation barrier on intact basal planes due to the chemical inertness. Self-assembled graphene flake films have 10X conductivity after selective platinum (Pt) ALD. In addition, a graphene field effect transistor (FET) model system is used to monitor graphene carrier density and mobility variation after ALD growth. Selective ALD of other conductive materials is also discussed.

Introduction

Defects in 2-D materials are a vital aspect of their electrical and mechanical properties. Graphene grown by chemical vapor deposition (CVD) unavoidably contains structural defects like grain boundaries and dislocations. Exfoliated graphene from Highly Ordered Pyrolytic Graphite (HOPG) can't avoid macroscopic defects such as folds, cracks, wrinkles which occur during CVD graphene transfer process. These defects all lead to scattering of charge carriers, which hinders electrical transport across the surface and limit the mechanical strength and stability of the graphene, and thus decreases the performance and reliability of related devices.

Atomic layer deposition enables film deposition with monolayer thickness control even over the most demanding topography. Furthermore, it can be material-selective, nucleating immediately on some surfaces but exhibiting a significant nucleation barrier on others (1, 2). The ideal graphene basal plane is composed of sp^2 hybridized carbon atoms linked to one another in a 2D honeycomb lattice with high electron-density in its aromatic rings. Together with the high C–C bond energy (4.9 eV), the repelling field from delocalized π-orbitals results in chemical inertness of graphene basal planes, which allows graphene to be the thinnest impermeable membrane(3). Defect sites of graphene (line, point, and boundary) are considerably more reactive, providing an opportunity for selective ALD deposition of very thin

conducting layers to improve conductivity across graphene defect sites (4). Bent et al. explored the nucleation behavior of Ru and Pt on Si (5) and CVD graphene (6). In addition, there are several reports about selective Al_2O_3 ALD on CVD graphene(7) and its application as corrosion resistant coating(8, 9). However, there remains a lack of research focused on improving the conductivity of solution-based printed graphene thin films by selective deposition of conductive materials.

Here, we use selective Pt ALD process to demonstrate a novel nanomanufacturing method for improving graphene thin film conductivity. To be specific, Pt is selectively deposited and grown at flake peripheral boundaries, thus stitching nearby graphene flakes together electrically, and over possible point and line defects in graphene flakes, thus healing the defects. (Fig. 1) Therefore, by combining graphene flake assembly with ALD healing and stitching, we produce conductive paths around and across the electrical defects so that the benefits of the pristine graphene regions are realized.

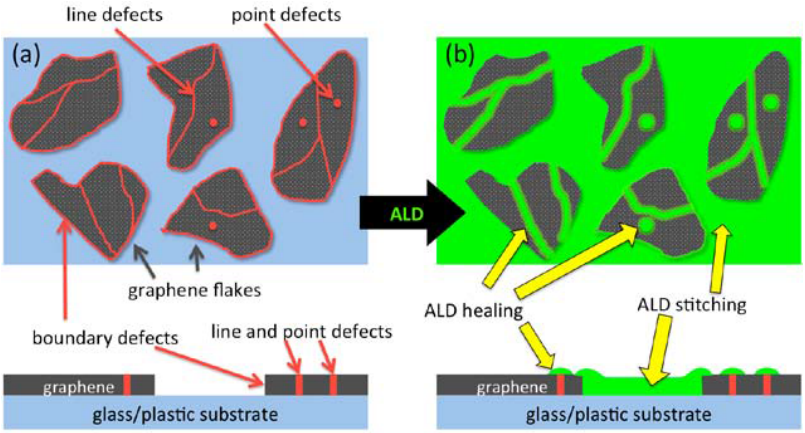


Figure1. (a) Separated graphene flakes on substrate, with red indicating line and point defects within graphene flakes, and boundary defects at graphene flake periphery. (b) Selective ALD provides conducting paths to heal point and line defects and to stitch flakes together while connecting at flake boundaries.

Experiment Methods

The graphene flake films tested in this study were self-assembled using a previously published technique(10). A solution of exfoliated graphene flakes suspended in N-Methyl-2-pyrrolidone (NMP) was injected into a petri dish containing 40mL of deionized (DI) water with a layer of 4mL of ethyl acetate floating on the surface of the water. The assembly of the loosely connected monolayer of graphene flakes was driven by desolvation from the NMP as well as convective plumes in the water created by the evaporation of the NMP. The glass substrates were coated by simple dip coating and dried in an oven at 120C for several hours.

To fabricate the graphene transistor device, we spin coated around 200nm PMMA on Si wafers with 300nm thermal oxide layers, then exfoliate graphene sheets from Kish graphite (11) on PMMA coated wafers. With the assistance of alignment windows, we use XYZ micromanipulator stages for careful alignment of the shadow mask to identified graphene sheets, and then place the whole assembly in a Metra Thermal Evaporation chamber for 50nm Au electrode deposition.

Pt ALD process using trimethyl(methylcyclopentadienyl)platinum(IV) ($MeCpPtMe_3$) and O_2 at 270°C were carried out in Cambridge Nanotech Fiji F200 with 1s $MeCpPtMe_3$ pulse time and 10s O_2 expose time at flow rate of 200sccm. The growth rate on Al_2O_3 and native Silicon oxide surface is ~ 0.4 Å/cycle.

Scanning electron microscopy (SEM) characterization was conducted using a Hitachi SU-70 analytical SEM with Energy-dispersive X-ray spectroscopy (EDS) capability. The electrical properties of the thin films were measured by Keithly 2400.

Results and Discussion

Electrically connecting separated graphene flakes

We demonstrate electrically stitching disconnected graphene flakes and healing defects on each flake. The ability to heal self-assembled films of solution-processed graphene flakes is important because of the ease and scalability of this technique in contrast to the synthesis and transfer of CVD graphene. Fig. 2a and 2b illustrate that Pt selectively nucleates on graphene edges and defects and provide electrical pathways around and across them, while Pt on glass substrate creates a conducting network connecting detached graphene flakes. The graphene basal plane is hydrophobic and inert, whereas dangling bonds at the periphery of the graphene flakes are more reactive, particularly to ligands on the ALD precursors (e.g., $-CH_3$, -OH and -COOH), driving dissociative precursor chemisorption at the graphene edge sites to accomplish selective deposition at defects. The sheet resistance evolution of a self-assembled film of graphene flakes on a quartz substrate was monitored by a four point probe station connected to a Keithley 2400 after various Pt ALD cycle numbers (Fig. 2c). A film of largely disconnected defective graphene flakes with sheet resistance of ~ 40kΩ/square achieves 10X conductivity improvement after 250 cycles of Pt to reach ~3kΩ/square. It is important to note that 250 cycles of Pt ALD on glass alone is almost insulating, demonstrating the synergistic effect of selective deposition and a preexisting broken conductive network with reactive sites. This proof of concept will be expanded to more economical conductive materials in future work.

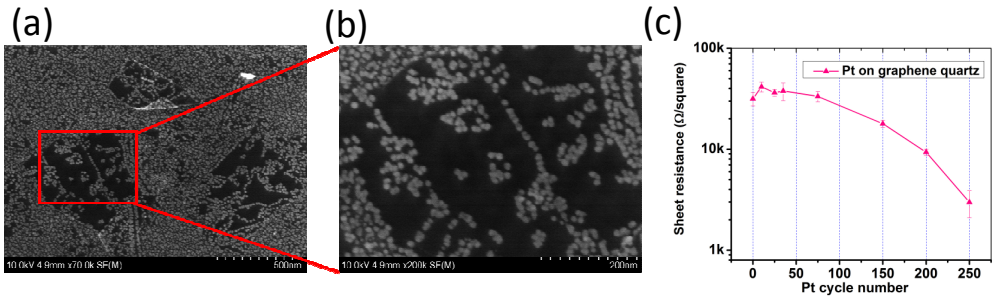


Figure 2. Pt ALD improves electrical properties of graphene flake thin film. (a) Separated graphene connected by Pt deposited on quartz substrate. (b) Zoomed-in image of one graphene flake in (b), showing Pt selective growth on defects and edges. (c) Sheet resistance of graphene decreases with respect to different ALD cycles.

Improving conductivity of an individual graphene flake

Besides connecting disjointed graphene flakes, selective ALD growth of Pt on the edges and defects may also benefit the conductivity of an individual graphene flake. In order to study the electrical properties of a single graphene flake, we adopted a lithography-free technique(12) to fabricate a graphene field effect transistor by shadow mask evaporation on exfoliated graphene, which can avoid surface contamination from photo or e-beam resist, leaving a pristine graphene surface intact for selectivity investigation. Another major challenge is possible shorting of device electrodes after ALD process on common insulating oxide substrates (eg. SiO_2, Al_2O_3), which are –OH terminated and reactive to ALD precursors. Poly (methyl methacrylate) (PMMA) films has shown growth-inhibiting behavior for various noble metal processes and metal oxides.(13) Therefore, we spin coated a PMMA onto SiO_2 substrate to prevent growth and avoid electrode shorting.

Using a two terminal measurement, source-drain current (I_{sd}) of the device is recorded between electrode 1 and 2 at room temperature with 10mV bias as a function of back gate voltage V_g, which controls the type and density of charge carriers. (Fig. 3d) I_{sd} at V_g=0V increases after Pt ALD, showing conductivity improvement. The decrease of I_{sd}-V_g curve slope after the selective Pt ALD process indicates reduced electron mobility compared to pristine graphene, which is reasonable as Pt nano clusters may introduce more electron scattering. Besides, the Dirac point shifts from 12.6V to more than 25V, suggesting p-doping of the graphene from Pt, which can be explained by the high work function of Pt (6.35eV) compared to graphene (4.4eV) leading to electron transfer from graphene to Pt. As the gate voltage is swept from negative to positive and backwards, a pronounced hysteresis behavior is observed, as designated by the arrows denoting the sweeping direction. It may originate from charge transfer between graphene and Pt nano particles or charge injection into trap sites on the

PMMA dielectric substrate.

Besides Pt reported in this paper, various ALD processes for other earth abundant and cost effective metals and conductive compounds are also available, such as titanium nitride, nickel (14), tungsten (15, 16) and transparent conductor aluminum doped zinc oxide (AZO), which may have promising applications in graphene manufacture.

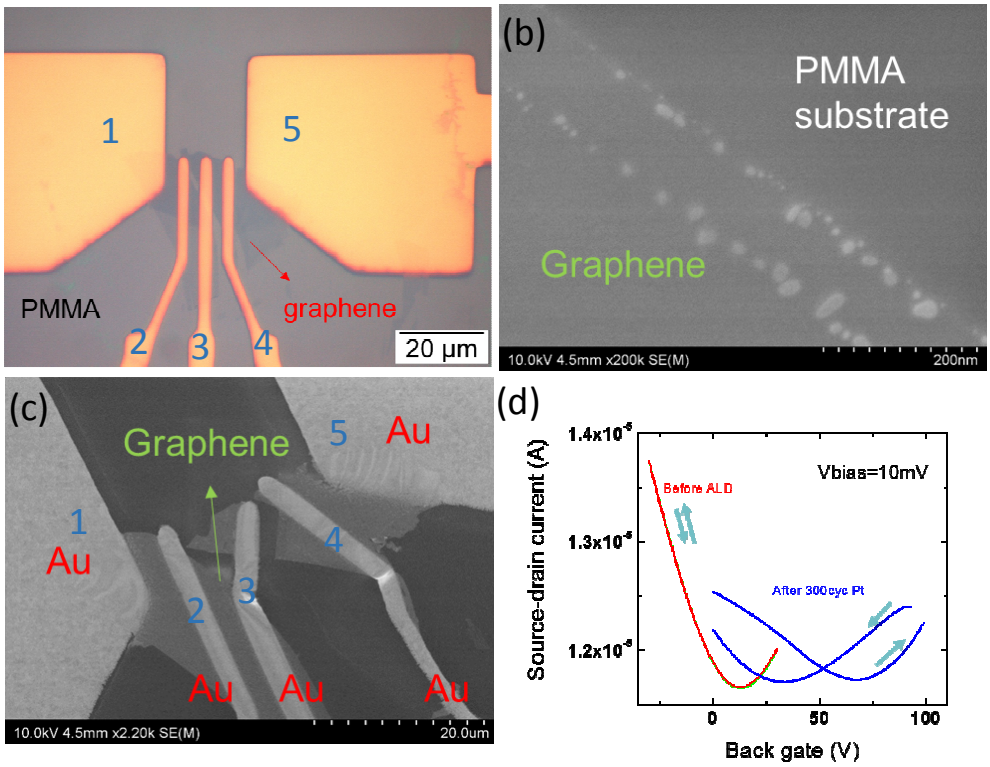


Figure 3. (a) Optical image of transistor made from pristine exfoliated graphene on PMMA coated SiO_2, with 5 Au electrodes. (b) SEM image of graphene after 300 Pt ALD cycles, showing selective growth at graphene step edges. (c) Electrode 3 and 4 curved after Pt ALD process. (d) Source-drain current vs. back gate voltage between electrode 1 and 2.

Conclusions

In summary, we demonstrated selective ALD growth on graphene defects and boundaries with various ALD processes for conductive materials (AZO and Pt). Selective ALD of Pt on structural defects present on graphene and over the blank area between graphene flakes leads to 10X conductivity of a graphene flake thin film. Conductivity improvement and doping effect from Pt ALD on a single graphene flake is also demonstrated by a back-gated graphene FET.

Acknowledgements

This work has been supported by the National Science Foundation (NSF) under Award Number 1300361. The authors also wish to acknowledge support of the Maryland Nanocenter.

References

1. X. Jiang, S. F. Bent, *The Journal of Physical Chemistry C* **113**, 17613 (2009).
2. M. N. Mullings *et al.*, *Journal of the Electrochemical Society* **157**, D600 (2010).
3. V. Berry, *Carbon* **62**, 1 (2013).
4. X. Wang, S. M. Tabakman, H. Dai, *Journal of the American Chemical Society* **130**, 8152 (2008).
5. S. M. Geyer, R. Methaapanon, B. Shong, P. A. Pianetta, S. F. Bent, *The Journal of Physical Chemistry Letters* **4**, 176 (2012).
6. K. Kim *et al.*, *Nature Communications* **5**, (2014).
7. D. Van Lam *et al.*, *Nanoscale*, **6**, 5639 (2014).
8. A. I. Abdulagatov *et al.*, *ACS Applied Materials & Interfaces* **3**, 4593 (2011).
9. Y. P. Hsieh *et al.*, *Acs Nano* **8**, 443 (2014).
10. J. Shim *et al.*, *Nano Letters* **14**, 1388 (2014).
11. K. S. Novoselov *et al.*, *Proceedings of the National Academy of Sciences of the United States of America* **102**, 10451 (2005).
12. W. Z. Bao *et al.*, *Nano Research* **3**, 98 (2010).
13. E. Farm, M. Kemell, M. Ritala, M. Leskela, *Journal of Physical Chemistry C* **112**, 15791 (2008).
14. W.-H. Kim *et al.*, *Journal of the Electrochemical Society* **158**, D1 (2011,).
15. W. Lei *et al.*, *Journal of Vacuum Science & Technology B* **24**, 780 (2006).
16. R. K. Grubbs, N. J. Steinmetz, S. M. George, *Journal of Vacuum Science & Technology B* **22**, 1811 (2004).